MEASUREMENTS OF DISTRIBUTED STRAIN DURING IMPACT PILE DRIVING

R.M Buckley[1], B.W. Byrne[1], J.P. Doherty[2], R.J. Jardine[3], S. Kontoe[3], R.A.McAdam[1], M.F. Randolph[2]*

[1] Department of Engineering Science, Oxford University, Parks Road, Oxford, UK
[2] Faculty of Engineering and Mathematical Science, University of Western Australia, 35 Stirling Highway, Perth, Australia
[3] Department of Civil and Environmental Engineering, Imperial College London, South Kensington, London, UK
** Corresponding author*

ABSTRACT This paper reports the use of optical Fibre Bragg Grating (FBG) sensors to monitor the stress waves generated below ground during pile driving, combined with measurements using conventional pile driving analyzer (PDA) sensors mounted at the pile head. Fourteen tubular steel piles with a diameter of 508 mm and embedded length to diameter ratios of 6 to 20 were impact driven at an established chalk test site in Kent, UK. The pile shafts were instrumented with multiple FBG strain gauges and pile head PDA sensors, which monitored the piles' responses under each hammer blow. A high frequency (5 kHz) fibre optic interrogator allowed a previously unseen resolution of the stress wave propagation along the pile. Estimates of the base soil resistances to driving and distributions of shaft shear resistances were found through signal matching that compared time series of pile head PDA measurements and FBG strains measured below ground surface. Numerical solutions of the one-dimensional wave equation were optimised by taking account of the data from multiple FBG gauges, leading to significant advantages that have potential for widespread application in cases where high resolution strain measurements are made.

Notation

A	Net cross-sectional area of pile (steel)
c	Wave speed in pile = $\sqrt{E/\rho}$
D	Pile diameter
E	Young's modulus of pile
F	Force in pile
F_d	Force in pile due to upward travelling wave
F_{max}	Maximum average measured force
F_{up}	Force in pile due to upward travelling wave
$F_{up,max}$	Maximum PDA force in pile due to upward travelling wave
f_s	Sleeve friction
G	Shear modulus of chalk
G_{max}	Maximum (small strain) shear modulus of chalk
G_1	Secant shear modulus of chalk
L	Pile embedded length
n	Number of strain gauge horizons
q_{ave}	Cone resistance averaged using the recommendations of Power (1982)
Q_b	Base resistance
R	External pile radius
R_i	Internal pile radius
R*	Equivalent radius of an open-ended pile = $\sqrt{(R)^2 - (R_i)^2}$
t	Time
t_{wall}	Wall thickness of the pile
t_{50}	Time for 50% pore water pressure dissipation
u_1	Pore water pressure in a CPT test measured at the cone tip
u_2	Pore water pressure in a CPT test measured at the shoulder
α	Viscous parameter
ε	Strain
ζ	Overall normalised error
ζ_f	Average root mean square error between the measured and calculated F at each strain gauge
$\zeta_{f,up}$	Average root mean square error between the measured and calculated F_{up} at the pile head
τ	Shaft shear friction

1. Introduction

Distributed strain during pile load testing has been measured previously using Fibre Bragg grating (FBG) sensors e.g. on large diameter concrete piles (Schmidt-Hattenberger *et al.*, 2003), jacked piles Liu and Zhang (2012) bored piles (Lee *et al.*, 2004, Schilder *et al.*, 2013) and driven piles (Byrne *et al.* (2019), McAdam *et al.* (2019)). FBGs have high strain competencies combined with high sampling rate capabilities that makes them suitable to capture the distributed strain response along the pile during impact pile driving. While several authors report the use of fibre optics to measure distributed strain during pile driving e.g. Baldwin *et al.* (2002), Byrne *et al.* (2019), McAdam *et al.* (2019), Schilder *et al.* (2013), Tran *et al.* (2011), the sensors are typically monitored at rates of <1kHz, which while relatively fast, cannot provide high resolution records of the travelling stress waves.

FBGs are sections of an optical fibre that have been laser etched with a grating of a given period. The grating period is strain and temperature dependent; light with a wavelength corresponding to the grating period is reflected while all other wavelengths pass the grating undisturbed. The change in wavelength of light reflected from the grating can be used to obtain the change in strain. The measured strain ε can be converted to force F at each sensor:

$$F = EA\varepsilon \qquad (1)$$

where E is the Young's modulus and A is the cross-sectional area. Under axial loading, measurements at multiple points along the pile length under load can be used to obtain the base resistance and the distribution of shaft stress, in a similar manner to conventional strain gauges. In a laterally loaded pile, the forces can be used to assess the soil-structure interaction during lateral loading.

Chalk is a generally structured very fine-grained porous weak carbonate rock, often encountered onshore in Northern Europe

as well as during offshore oil, gas and wind-energy installations. Large open-ended driven piles are employed for most offshore and near-shore developments (Lord *et al.* (2002), Jardine *et al.* (2018), which present difficulties to designers in these highly variable materials. Recent research has aimed to advance the understanding of the axial behaviour of displacement piles in chalk (Buckley *et al.*, 2018a, Buckley *et al.*, 2018b, Ciavaglia *et al.*, 2017a, b) and has led to new preliminary design rules for axial pile design (Buckley, 2018, Buckley *et al.*, 2020a, Jardine *et al.*, 2018)

The ALPACA JIP (Axial-Lateral Pile Analysis for Chalk Applying multi-scale field and laboratory testing Joint Industry Project), described by Jardine *et al.* (2019) is underway to investigate a wide range of axial and lateral cyclic loading conditions through high quality experiments on driven piles. Fourteen of the piles were instrumented before driving with novel fibre optic strain gauge sensors embedded along their shaft, as well as above ground pile driving analyzer (PDA) strain gauges and accelerometers. This paper describes the installation and dynamic load testing of the main set of 508mm diameter open-ended tubular steel piles. The PDA and FBG measurement frequencies were sufficiently high to: (i) allow the stress waves travelling in the pile during each hammer impact to be tracked during pile installation; (ii) allow novel comparisons to be made between the distributed forces along the pile, as measured by the FBG instruments, and those assessed from the PDA data using one-dimensional stress wave theory; and (iii) develop an optimisation process to improve the match between measured and calculated distributed forces.

2. Test site

The test site is in a chalk quarry test site located close to the village of St. Nicholas at Wade, Kent, UK (UK Grid TR 25419 66879). The site has been used previously to advance understanding of displacement piles in chalk (Buckley *et al.*, 2018a, Buckley *et al.*, 2018b, Ciavaglia *et al.*, 2017a, b). The ground conditions at the site are described by Buckley *et al.* (2020b). The chalk at the site classifies as low-medium density (IDD = 1.38 to 1.64Mg/m^3) structured Grade B3-A2 material with small to medium-sized flints, within the current classification system (Bowden et al., 2002). Although the water table is located at ≈6m below ground level the degree of saturation above this is between 90 and 100%. Figure 1 shows a typical CPT profile from the site. The corrected cone resistance q_t varies typically from 10-20MPa above 8m depth increasing to between 10 and 30MPa with depth. Sleeve friction, f_s is typically between 200 and 500kPa and increases slightly with depth. Excess pore water pressures (not shown) are remarkably high, ranging from 2 to 6MPa at the shoulder (u_2) position and up to 12MPa at the tip (u_1) position. During dissipation tests, times for 50% porewater pressure dissipation t_{50} of between 2 and 4 seconds were observed. Figure 1 shows the range of shear modulus (G_{max} or G_{vh}) obtained from seismic CPT (SCPT) measurements. The shear modulus typically ranges from 700 to 2400MPa, with significant scatter observed in near surface measurements.

Figure 1 CPT and SCPT profiles from the site

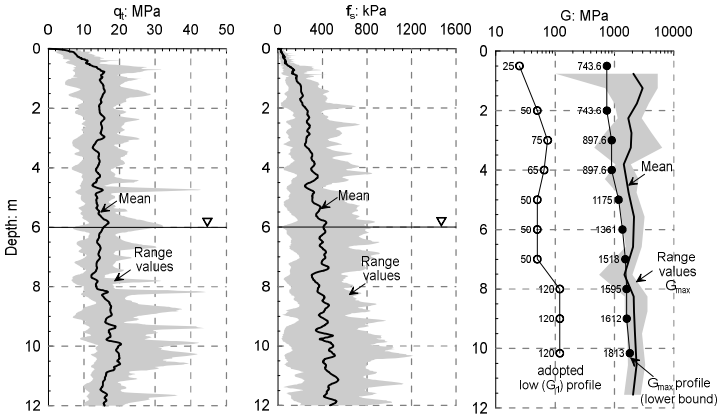

3. Test piles and instrumentation

A total of 14 508mm diameter open-ended tubular steel (API 5L Grade X80) piles, with a wall thickness ≈20.6mm were driven at the site using a Junttan SHK 100-3 4T hydraulic impact hammer. Figure 2 shows the pile layout plan. The embedded length to diameter ratios (L/D) of the piles ranged from 6 to 20 with two of the piles installed to 3.05m and the remaining twelve piles installed to 10.16m depth. The piles were driven at rates of between ≈1-2 blows per second and were all fully coring during installation. A driving 'dolly' was used to ensure that the internal chalk column did not come into contact with the hammer and cause an undesirable pile driving interruption.

Figure 2 Pile layout plan

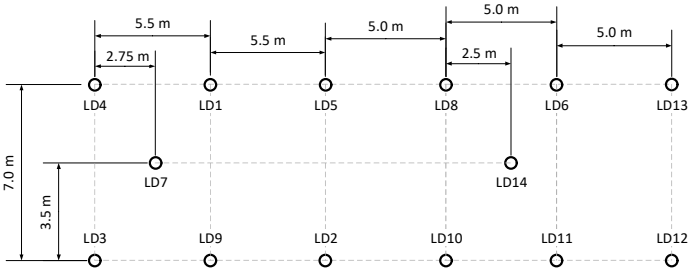

Strain gauges and accelerometers were attached near the pile head to give information on the force and velocity at the pile top for each hammer blow. The PDA measurements were sampled at a frequency of 40kHz to obtain a detailed time history for each blow. The FBG instrumentation was installed by Marmota Engineering in pre-cut 5mm square grooves. Each groove included 12 strain gauges in one string, a number selected based on the bandwidth of the Micron Optics si155 interrogator. LD01 to LD13 were each instrumented with diametrically opposite strings of 12 FBG sensors spaced as shown in Figure 3. LD14, which was used in a subsequent multi-directional lateral loading test, was instrumented with four strings spaced circumferentially around the pile, each including an FBG temperature sensor close to the bottom strain sensor. The FBGs were logged continuously at a sampling frequency of 5kHz (the highest sampling rate offered by an interrogator at the time of driving).

Figure 3 Layout of instrumentation on the test piles

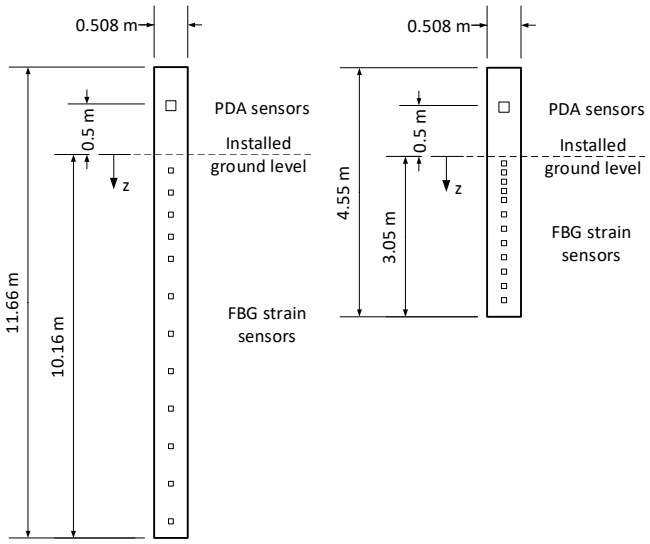

4. Pile driving results

4.1 Dynamic monitoring

In driving stress-wave analysis, measured accelerations are integrated to give time series of pile velocity, v, and displacement. The strains, ε, measured by the PDA gauges are used to obtain the forces. A numerical method, such as the method of characteristics (Middendorp, 1987) is used to solve the one-dimensional wave propagation equation. The measured F or Zv (where Z is the pile impedance EA/c with EA the cross-sectional stiffness of the pile and c the wave propagation speed) signals can be used as the input boundary condition. The two signals may also be combined to obtain the downward travelling component of the stress-wave, fitting the numerical solution to the upward travelling component. The static and dynamic soil or rock resistances affect the reflected traces from below ground level and simplified rheological models are used to simulate their effects by applying combinations of springs, dashpots and plastic sliders.

A schematic of the downward travelling wave $F_d=(F+Zv)/2$ and measured reflections at the PDA gauges at the pile top is shown on Figure 4 along with the upward travelling force, $F_{up}=(F-Zv)/2$ calculated from the end of driving (EOD) blow. Taking a steel mass density of 7.8Mg/m^3 and Young's modulus E of 210GPa gives a pile impedance Z of 1277kNs/m.

Figure 4 Schematic of stress waves travelling in a pile

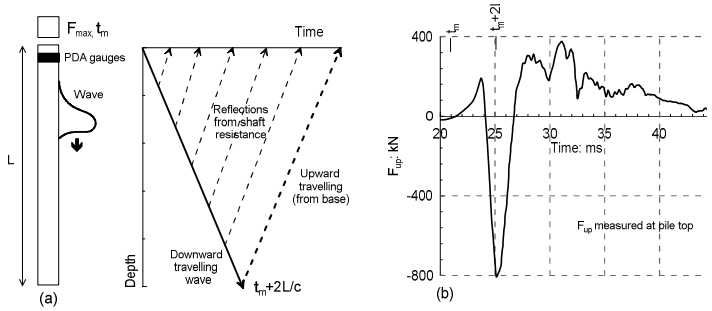

4.1 Optical fibre Bragg grating measurements

Figure 5 shows the time history during all the 832 driving blows required to install pile LD05 (L/D=20), in terms of the force calculated from the average strain at the top gauge level from the two diametrically opposite fibre optic strings. A number of seating blows were applied initially followed by a pause to check the verticality of the pile. As is shown on Figure 5, a 'zero drift' (or non-zero measurement) in FBG strain was observed after most blows, which was seen at all gauge levels, in both tension and compression. The residual forces observed may be a result of (i) locked-in stresses in the steel or groove which are 'shaken' down during pile driving and/or (ii) changes in strain due to changes in temperature. To aid interpretation, the strain at the beginning of each blow was zeroed at the start of each blow, as illustrated on Figure 6, which shows the strain time history for the EOD blow on pile LD05. This is considered appropriate since any locked-in stresses due to soil-pile interaction are small, relative to the stresses induced by the impact shockwave, as are the temperature variations over the short period of observation time for a hammer blow.

Figure 5 Time history for all 832 blows applied to LD05

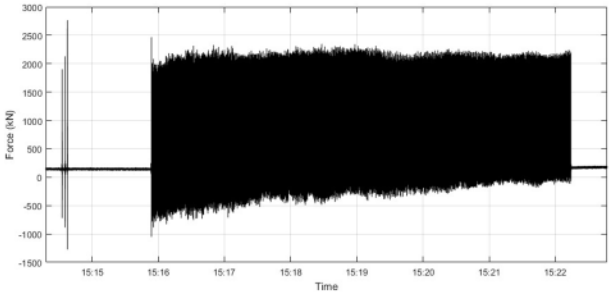

Figure 6 FBG strain-time histories under a single blow

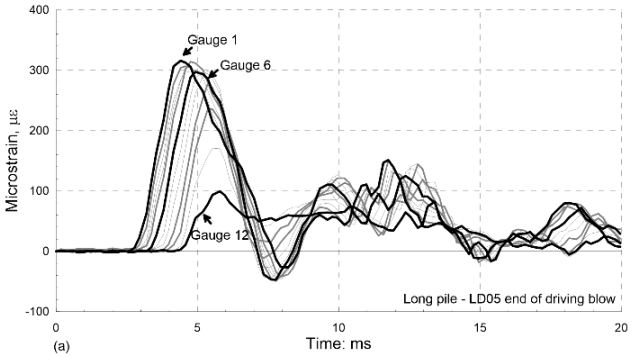

5. Analysis of dynamic measurements

Stress-wave matching was carried out using the research-oriented software program IMPACT (Randolph, 2008) which employs shaft and base resistance models based on elasto-dynamic theory. The parameters defining the resistance models were iteratively changed until a good match was obtained between the computed stress-wave (in this case the upward travelling wave, using the downward travelling component as input) and that deduced from the PDA data. This leads to base and shaft resistance assessments for each blow analysed. The

parameters include the shaft stress distribution, base resistance, chalk density, shear modulus, and shaft viscosity parameters, α and β. The chalk density and shear modulus were determined from the site investigation.

The adopted values of (secant) shear modulus were degraded from the very high small strain values recorded during the site investigation to account indirectly for non-linearity and the very soft annulus of putty that forms around the shaft during driving (Buckley *et al.*, 2018a). The shaft viscosity parameters, α and β were adopted as 1.1 and 0.2 respectively and the pile tip resistance was taken as 0.6 times the cone resistance, q_t. The latter was averaged using the recommendations of Power (1982). Additional details on the analyses are provided by Buckley *et al.* (2020b). An example 'manual' signal match is shown on Figure 7 for the end of driving blow during installation of pile LD05.

Figure 7 Example signal match on pile LD05

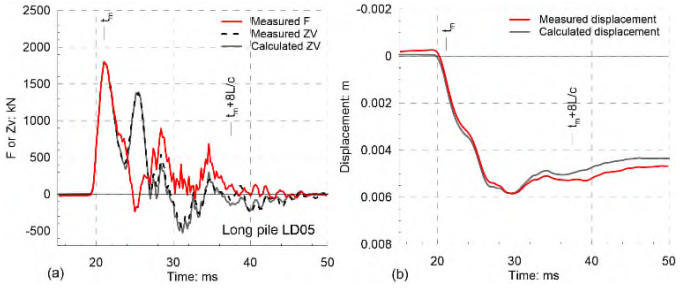

It is well established that the signal matching process does not lead to a unique solution; multiple similar parameter sets can provide similar degrees of fit to the measured data and lead to subjective results (Fellenius, 1988). In this case, the FBG measurements can be used to match the forces calculated by IMPACT at twelve additional nodes, which further constrains the possible solutions. The forces measured at the top and bottom gauges at the end of driving, along with the calculated force from IMPACT are shown on Figure 8 for the example LD05 case. The corresponding match to the PDA data was shown previously on Figure 7. Although good agreement is observed between the measured and calculated force time histories, which gives confidence in the proposed trial signal matching parameters, the forces recorded by the FBG bottom gauge are less reliably predicted.

Figure 8 Example measured force from below-ground FBGs with forces calculated using IMPACT

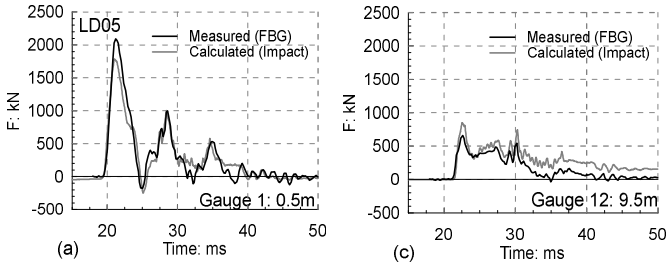

To improve the matches shown in Figure 8, an automated optimisation procedure was developed to search for the shear resistance values which led to the lowest magnitude of difference between the measured and calculated forces. The accuracy of an overall individual match was quantified by comparing normalised values of the measured and calculated error. The overall normalised error is expressed as:

$$\zeta(\%) = 0.5 \times \frac{1}{n}\sum_{i=1}^{n}\frac{\zeta_f(i)}{F_{max}(i)} + 0.5 \times \left(\frac{\zeta_{f,up}}{F_{up,max}}\right) \quad (2)$$

where n is the number of strain gauge horizons and ζ_f is the average root mean square error between the measured and calculated force at each strain gauge horizon, F_{max} is the maximum force measured at each strain gauge $\zeta_{f,up}$ is the average root mean square error between the measured and calculated upward force at the pile head and $F_{up,max}$ is the maximum measured upward force at the pile head. The distribution of shaft resistance is varied, whilst the viscosity parameters, shear modulus and base resistance were kept as in the manual matches. The following cases are considered as shown on Figure 9:

1. Using just the PDA data as input i.e. optimising an objective function using the second term in (2).
2. Using both the PDA and FBG data as input, optimising using both terms in (2).

The shear resistance (τ) values were allowed to vary non-uniformly with depth between bounds of $0<\tau<300$ kPa using the Matlab patternsearch function. The initial estimate was based on the manual signal matching analysis results. The normalised error, calculated using (2) was 6.0% for the manual match presented in Figures 7 and 8, which reduced to 5.0% for optimisation using the PDA input only and further to 4.1% for the case using the PDA and FBG input together. The results indicate that in all cases, the overall normalised error is reduced significantly by the optimisation process. Additional optimisation of the viscosity parameters, α and β, and the shear modulus was explored and is discussed by Buckley *et al.* (2020b). Figure 9 shows two examples of the resulting shear resistance profiles from the optimisation, when the pile tip was at (i) 7.6m below ground level and (ii) at the final penetration depth of 10.16m.

Figure 9 Profiles of shear stress from optimisation

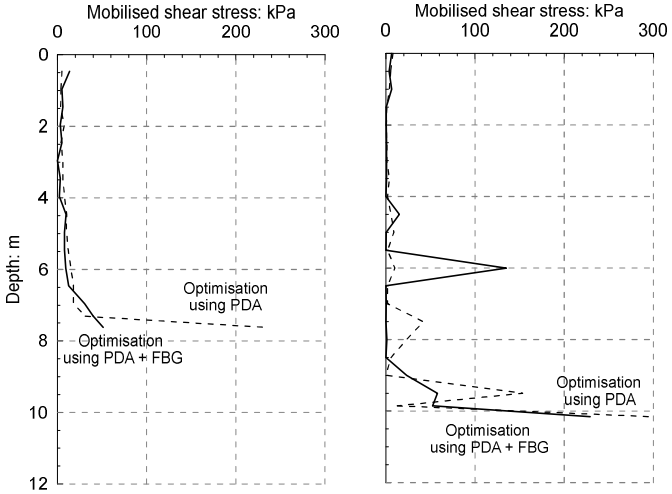

Figure 10 shows examples of the measured and optimised calculated force time histories (from case 2) for two gauge levels along the shaft for pile LD05 at EOD, which show significant improvements over Figure 8.

Figure 10 Examples of FBG forces measured below-ground FBGs and optimised IMPACT signal matches

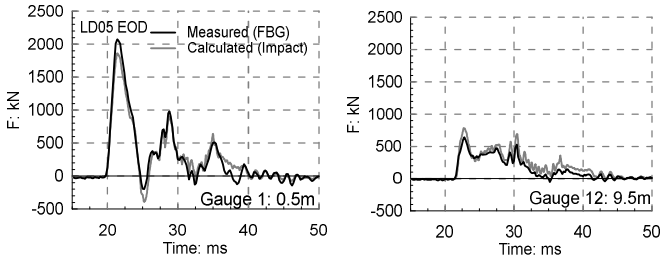

The spike in mobilised shear stress at a depth of 6m (see Figure 9), which also appeared from optimisation of the fit to the penultimate blow (not shown here), appears to be a spurious artefact of the FBG data, due to either (i) small timing errors in the signals, (ii) the effects of residual strains that have been zeroed out or (iii) the limited strain resolution available with the relatively thick-walled test piles.

A sharp tendency for the local shaft shear stress to attenuate with increased pile penetration (known as 'friction fatigue' or the mh/R* effect) is evident from Figure 8. A similar trend has been observed in low-medium density chalk by at other sites Buckley *et al.* (2020c). Figure 11 plots the local shear stress normalised by the average CPT cone resistance q_{ave} (Power, 1982) as a function of h/R^* (where h is the distance from the pile tip to any given soil horizon and $R^*=\sqrt{R^2-R^2_i}$, with R and R_i being the external and internal pile radii respectively), during driving of pile LD02 which, similar to LD05, also had an L/D ratio of 20. Nine optimised blows are included on this figure including the final driving blow (1113). The qualitative trend of strongly reducing τ/q_{ave} with increasing h/R^* is evident, although unexpected spikes in the measurements are still observed (e.g. blow 1113) which are attributable to the measurement issues described above.

Figure 11 Optimisation of blows for pile LD02

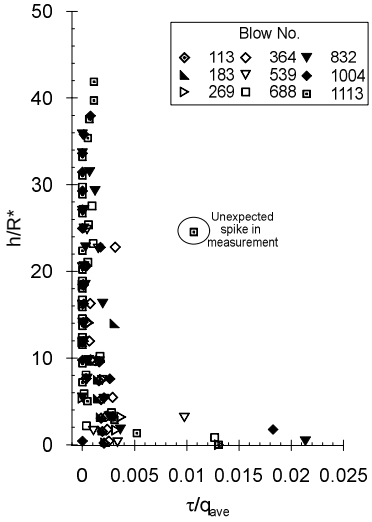

8. Conclusion

This paper has described the interpretation of FBG measurements taken on 508mm diameter tubular steel piles (L/D = 6 to 20) during impact driving at a well-characterised test site in Kent, UK. High frequency measurements taken with the pile head PDA and pile shaft FBG sensors allowed detailed analysis of the signals recorded during the driving of each pile. The analysis has shown the advantages of combining PDA and FBG measurements and a process to optimise the signal matching process with both sets of measurements. Changes in the residual strain measurements were removed after each blow during driving, which meant that any true residual locked in forces were eliminated. The relatively high wall thickness of these piles led to lower than ideal axial strain resolutions. However, these effects would be greatly reduced when considering long piles with lower diameter-to-wall thickness ratios. In these cases, the FBG force measurements would be very valuable, particularly in layered profiles.

9. Acknowledgements

The ALPACA Project was funded by the Engineering and Physical Science Research Council (EPSRC) through grant EP/P033091/1. The Authors acknowledge the provision of additional financial and technical support by the following project partners: Atkins, Cathies, Fugro, GCG, innogy, LEMS, Ørsted, (formerly DONG Energy), Parkwind, Siemens, SPR and Equinor (formerly Statoil). The Authors acknowledge gratefully the work of Socotec UK Ltd (formerly ESG) as the main contractor for the field testing programme, Marmota Engineering AG as the subcontracted fibre optic strain gauge specialist, Green Piling Ltd who installed the piles, and Lankelma UK and Fugro Geo-services who carried out the boreholes and cone penetration tests respectively. The Authors are also grateful to Mr. Ken Vinck who helped to supervise the site investigation.

10. References

Baldwin C. S., Salter, T., Niemczuk, J. B., Chen, P. C. & Kiddy, J. S. (2002). Structural monitoring of composite marine piles using multiplexed fiber Bragg grating sensors: In-field applications. *Smart Structures and Materials 2002: Smart Systems for Bridges, Structures, and Highways*: 82-91.

Bowden A. J., Spink, T. W. & Mortimore, R. N. (2002). The engineering description of chalk: its strength, hardness and density. *Q. J. Eng. Geol. Hydrogeol.*, **35**, No. 4: 355-361.

Buckley R. M., Jardine, R. J., Kontoe, S., Parker, D. & Schroeder, F. C. (2018a). Ageing and cyclic behaviour of axially loaded piles driven in chalk. *Géotechnique*, **68**, No. 2: 146-161.

Buckley R. M., Jardine, R. J., Kontoe, S. & Lehane, B. M. (2018b). Effective stress regime around a jacked steel pile during installation ageing and load testing in chalk. *Can. Geotech. J.* , **55**, No. 11: 1577-1591.

Buckley R. M. (2018). *The axial behaviour of displacement piles in chalk*. PhD Thesis, Imperial College London, London, UK.
Buckley R. M., Jardine, R. J., Kontoe, S., Barbosa, P. & Schroeder, F. C. (2020a). Full-scale observations of dynamic and static axial responses of offshore piles driven in chalk and tills, *Géotechnique*, online ahead of print.
Buckley R. M., McAdam, R. A., Byrne, B. W., Doherty, J. P., Jardine, R. J., Kontoe, S. & Randolph, M. F. (2020b). Optimisation of impact pile driving using optical fibre Bragg grating measurements, *Under review*.
Buckley R. M., Kontoe, S., Jardine, R. J., Schroeder, F. C. & Barbosa, P. (2020c). Pile driveability in low to medium density chalk. *Under review*.
Byrne B. W., McAdam, R. A., Burd, H. J., Beuckelaers, W. J. A. P., Gavin, K., Houlsby, G. T., Igoe, D., Jardine, R. J., Martin, C. M., Muir Wood, A., Potts, D. M., Skov Gretlund, J., Taborda, D. M. G. & Zdravković, L. (2019). Monotonic lateral loaded pile testing in a stiff glacial clay till at Cowden, Géotechnique, *online ahead of print* https://doi.org/10.1680/jgeot.18.pisa.003.
Ciavaglia F., Carey, J. & Diambra, A. (2017a). Time-dependent uplift capacity of driven piles in low to medium density chalk. *Géotechnique Letters*, **7**, No. March: 1-7.
Ciavaglia F., Carey, J. & Diambra, A. (2017b). Monotonic and cyclic lateral tests on driven piles in Chalk. *Proc. of the ICE Geotech. Eng.*, **170**, No. 4: 353-366.
Fellenius B. H. (1988). Variation of CAPWAP results as a function of the operator. *Proc. 3rd Intl. Conf. on the Application of Stress Wave Theory to Piles*, Ottawa, Canada: 814-825.
Jardine R. J., Buckley, R. M., Kontoe, S., Barbosa, P. & Schroeder, F. C. (2018). Behaviour of piles driven in chalk. *Engineering in Chalk*. ICE Publishing: 33-51.
Jardine R. J., Buckley, R. M., Byrne, B., Kontoe, S., Macadam, R. & Vinck, K. (2019). The ALPACA research project to improve driven pile design in Chalk. *Proc. 17th European Conference on Soil Mechanics and Geotechnical Engineering*, Reykjavik, Iceland: 1-8.
Lee W., Lee, W.-J., Lee, S.-B. & Salgado, R. (2004). Measurement of pile load transfer using the Fiber Bragg Grating sensor system. *Canadian Geotechnical Journal*, **41**, No. 6: 1222-1232.
Liu J. & Zhang, M. (2012). Measurement of residual force locked in open-ended pipe pile using FBG-based sensors. *Electron. J. Geotech. Eng*, **17**, No.: 2145-2154.
Lord J. A., Clayton, C. R. l. & Mortimore, R. N. (2002). *Engineering in chalk*, CIRIA, C574.
McAdam R. A., Byrne, B. W., Houlsby, G. T., Beuckelaers, W. J. A. P., Burd, H. J., Gavin, K., Igoe, D., Jardine, R. J., Martin, C. M., Muir Wood, A., Potts, D. M., Skov Gretlund, J., Taborda, D. M. G. & Zdravković, L. (2019). Monotonic lateral loaded pile testing in a dense marine sand at Dunkirk, Géotechnique, *online ahead of print* https://doi.org/10.1680/jgeot.18.pisa.004.
Middendorp P. (1987). *Numerical model for TNOWAVE*, TNO-IBBC, Report BI-86-75.
Power P. (1982). The use of the electric static cone penetrometer in the determination of the engineering properties of chalk. *Proc. 2nd Eur. Symp. on Penetration Testing*, Amsterdam, The Netherlands: 769-774.
Randolph M. F. (2008). *IMPACT - Dynamic analysis of pile driving*, Manual.
Schilder C., Kohlhoff, H., Hofmann, D., Basedau, F., Habel, W. R., Baeßler, M., Niederleithinger, E., Georgi, S. & Herten, M. (2013). Static and dynamic pile testing of reinforced concrete piles with structure integrated fibre optic strain sensors. *Fifth European Workshop on Optical Fibre Sensors*, 2013. pp 879447.
Schmidt-Hattenberger C., Straub, T., Naumann, M., Borm, G., Lauerer, R., Beck, C. & Schwarz, W. (2003). Strain measurements by fiber Bragg grating sensors for in situ pile loading tests. *Smart Structures and Materials 2003: Smart Sensor Technology and Measurement Systems*, 2003. pp 289-294.
Tran K. T., McVay, M. C., Herrera, R. & Lai, P. (2011). A new method for estimating driven pile static skin friction with instrumentation at the top and bottom of the pile. *Soil Dynamics and Earthquake Engineering*, **31**, No. 9: 1285-1295.